Infrared Measurement of Base Metal Temperature in Gas Tungsten Arc Welding

Elimination of interfering radiation from the arc and tungsten electrode are found to be required for accurate infrared temperature measurements of base metal temperature

BY D. FARSON, R. RICHARDSON AND X. LI

ABSTRACT. Quantification of infrared (IR) radiation is a convenient, non-contact method for making the base metal temperature measurements needed for on-line feedback controls. However, the problem of interference from the arc is a complicating factor in applying IR temperature sensing to welding. The objective of this research is to implement and test a top-face, non-contact temperature measurement system based on optical pyrometry. Investigations relating to the development of an infrared temperature measurement system are described. An apparatus consisting of a fiberoptic cable, a silicon photodiode/power meter and a computer data acquisition system were configured and used for the tests. Results of the experiments showed that radiation from both the arc and the hot tungsten electrode were important sources of interference in the IR emissions from the base metal. Attenuation of the interfering radiation using a band-pass optical filter and a specially-designed gas cup was investigated. Finally, the sensing system was calibrated using thermocouple measurements of actual base metal temperature.

Introduction

Automation offers the potential to improve weld product quality and consistency. However, "hard" or "open-loop" automation requires repeatable preparation of parts. In practice, feedback control is often desired in automated welding systems to adapt for variations in raw materials (*i.e.*, fitup as well as weld parameter fluctuations). These general comments apply specifically to weld penetration — a very important factor affecting weld quality, since it is closely related to the structural integrity of welds. Major issues in the design and implementation of feedback weld penetration controls are weld process modeling, controller design and real-time penetration sensing methods. This research focused on the measurement of base metal temperature at a location near a gas tungsten arc welding (GTAW) pool. In subsequent research, these measurements were used in conjunction with a thermal model to produce real-time estimates of weld penetration for feedback control implementation. Because welding is physically complex and accurate real-time simulations are difficult to achieve, direct measurements of weld penetration would be more desirable than predictions. Occasionally, sensors that observe the back of the weld to directly measure penetration have been used successfully. For practical reasons, however, top-face non-contact measurements are usually required. The objective of this research was to implement and test a top-face non-contact temperature measurement system based on optical pyrometry.

D. FARSON, R. RICHARDSON and X. LI are with the Department of Industrial, Welding and Systems Engineering, The Ohio State University.

KEY WORDS

Arc Light
Band-Pass Optical Filter
Base Metal
GTAW
Infrared Radiation
Interference
Wavelengths

Background

Practical temperature measurement methods can be grouped into two categories: contact and non-contact. The three most common contact temperature transducers — thermocouples, RTDs and thermistors — must be well-coupled to the target because they essentially measure their own temperature. They are generally inexpensive, but tend to have slow response speed (Ref. 1). Due to this and the requirement for good thermal contact with the target, they have been rarely used for practical real-time control implementation. Non-contact temperature measurements are accomplished by infrared (IR) thermometry. IR sensors usually have fast response and are commonly used to measure moving targets, targets in a vacuum and targets that are inaccessible due to hostile environments, geometry limitations or safety hazards (Ref. 1). Their cost tends to be high, although in some cases may be comparable to a contact device. In most welding process control applications, non-contact sensing is much better than contact sensing.

Infrared sensing systems measure temperature by quantifying the electromagnetic energy emitted by all materials at a temperature above absolute zero (0K). A basic design consists of a lens to focus the IR energy onto a detector, which then converts the energy to an electrical signal that can be displayed in units of temperature after being compensated for ambient temperature variation.

The IR part of the electromagnetic spectrum spans wavelengths from 0.7–1000 μm. Within this wave band, frequencies of 0.7–20 microns are usually used for practical temperature measurement. Planck is credited for developing the theoretical basis for IR temperature measurement, having derived an equa-

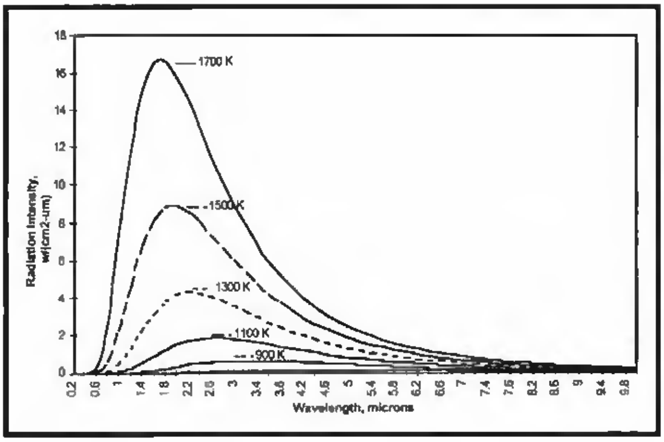

Fig. 1 — Planck's Law for a black body.

tion that expresses the spectral emissivity of a surface in terms of temperature and material properties (Ref. 1):

$$W_\lambda = C_1\, \varepsilon_\lambda [\lambda^5 (\mathrm{Exp}(C_2/\lambda T) - 1)]^{-1}$$

where

W_λ = spectral radiant intensity, W/(cm^2 – μm)
C_1 = 34,413 W – μm^4/cm^2
C_2 = 14,388 μm – K
ε_λ = emissivity
λ = wavelength, μm
T = temperature, K

A plot of the radiation intensity as a function of the wavelength and temperature for a black body (ε_λ = 1.0) according to Planck's Law is shown in Fig. 1. Note that emission below 1 micron is very small for temperatures less than about 900 K.

A calculated curve of spectral radiant intensity as a function of temperature at a 1000-nm wavelength is shown in Fig. 2. In this figure, temperature ranges from 200 to 2000°C (392 to 3632°F). The melting point of mild steel is about 1493°C (2717°F) and temperatures of interest in welding process control are typically between 500°C (932°F) and the melting point of the mild steel. From the curve, the radiation intensity is seen to increase rapidly with temperature. For example, the radiation intensity is about 0.00001 W/(cm^2 – μm) at 400°C (752°F), but is 0.1 W/(cm^2 – μm) at 800°C (1472°F). This wide variation limits the application of most common detectors for measuring this range of temperature.

It is important to understand the characteristics of radiation generated by the welding arc because it is a source of potential interference in temperature measurement. Welding arcs are complex sources of radiation because of their diverse atomic and molecular species. Prior studies of welding arc spectra have been conducted for the purpose of better understanding the physics of the welding arc and arc welding process control. Richardson (Ref. 2) performed flat position bead welds on mild steel bars with gas tungsten arcs with different shielding gas. He used a spectrograph to analyze arc radiation. A typical gas tungsten arc spectra is shown in Fig. 3. It can be seen from the spectra that the arc radiation is relatively low above a wavelength of 1000 nm. This suggests the use of a narrow bandwidth filter around the wavelength to block out arc light radiation when trying to measure the surface temperatures on the top face of a workpiece.

There have been previous reports of work dealing with infrared measurement of temperature in conjunction with arc welding. Infrared temperature sensing systems have also been used to monitor cooling rates in welds for on-line control of heat input (Refs. 3, 4) and for similar welding process control applications (Refs. 5–9). Unfortunately, some of these systems are sensitive to variations in material emissivity and arc light interference. For mitigating arc interference, arc interruption (*i.e.*, current pulsing) and external illumination methods have been applied (Refs. 10, 11). Nomura (Ref. 11) discussed the application of a silicon photodiode sensor to measure the base metal temperature on a welding line. This sensor was used for pulse GTAW (peak current: 300 A, base current: 5 A). The sensor signal was said to be corrupted by arc radiation during the high-current portion of the pulse, but could be calibrated to match the temperature measured by thermocouple during the low-current pulse (except for locations in front of the molten pool).

Experimental Apparatus and Procedure

A non-contact, top-face IR temperature sensing system for use with non-pulsed direct-current GTAW was designed and calibrated. The temperature-sensing system used a special gas cup, silicon photodetector, band-pass optical filter, fiber optic system (to transport light for remote detection) and a light power meter. A layout of the sensing system is shown in Fig. 4. The base metal sensing point was located 11 mm behind the weld pool and 5 mm to one side of the weld centerline. A focusing system collected the light from the sensing point with a divergence of up to a 23-deg full-cone angle from a 0.6 mm focused spot (on the work surface) at a distance of 40 mm. The focus head was mounted to the GTAW torch using a bracket. A laser-fiber illuminator system transmitted the collected light to a silicon photodiode detector operated at room temperature. The detector signal was connected to an optical power meter, which processed the signal and output to produce an analog signal proportional to optical power as output to a computer data acquisition system. A software program in the data acquisition computer was used to sample the output voltage of the optical power meter and to convert the voltage values into the optical power values.

Since radiation from the arc and the tungsten electrode would affect the temperature measurement by illuminating the sensing point (adding to surface emission), it was attenuated by a band-pass optical filter and a special gas cup. The band-pass optical filter had a central wavelength of 1064 nm and a range of 15.2 nm with 45% transmission. The special gas cup was designed to shadow the sensing point from arc and electrode radiation. Details concerning selection of the optical filter and the design of the gas cup will be discussed later.

To align the fiber optic system, a helium-neon laser was used to transmit light into the detector end of the fiber optic, which allowed illumination of the focal point of the collection optics. By adjusting the focusing system and the distance between the focused spot on the base metal and the focus head, the desired spot size and position on the base metal were obtained.

The welding experiments described in the following section were performed over a water-cooled copper anode, or as bead-on-plate welds in AISI 1250 sheet metal (noted in each case). The sheet metal weld coupons had dimensions of 152 × 63.5 × 3.2 mm (6 × 2.5 × 0.125 in.). To maintain consistent surface conditions and to minimize emissivity variations, all AISI 1025 sheet metals were mechanically cleaned by wire brushing. Plates were then put into a mixture of 60% water, 30% acetone and 10% nitric acid for 30 min. Afterward, the metal was rinsed with water and dried. By visual inspection, the parts appeared to have relatively high and uniform emissivity after

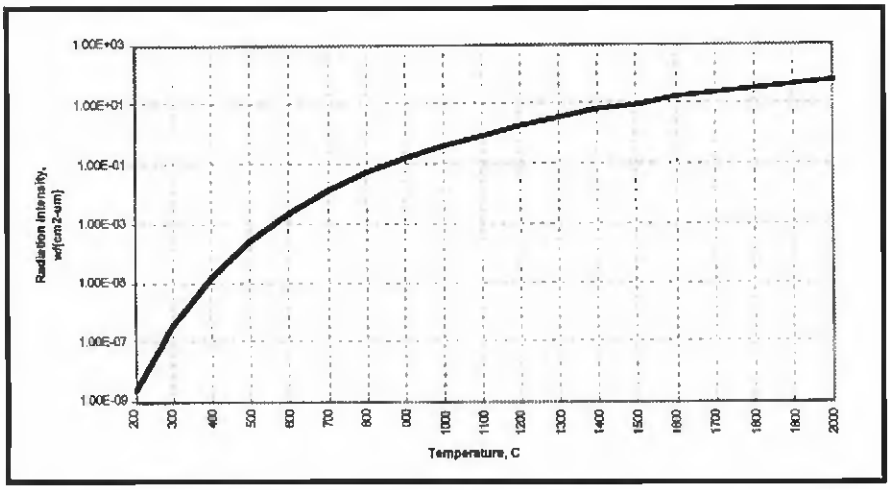

Fig. 2 — Radiation intensity at 1000 nm as a function of temperature.

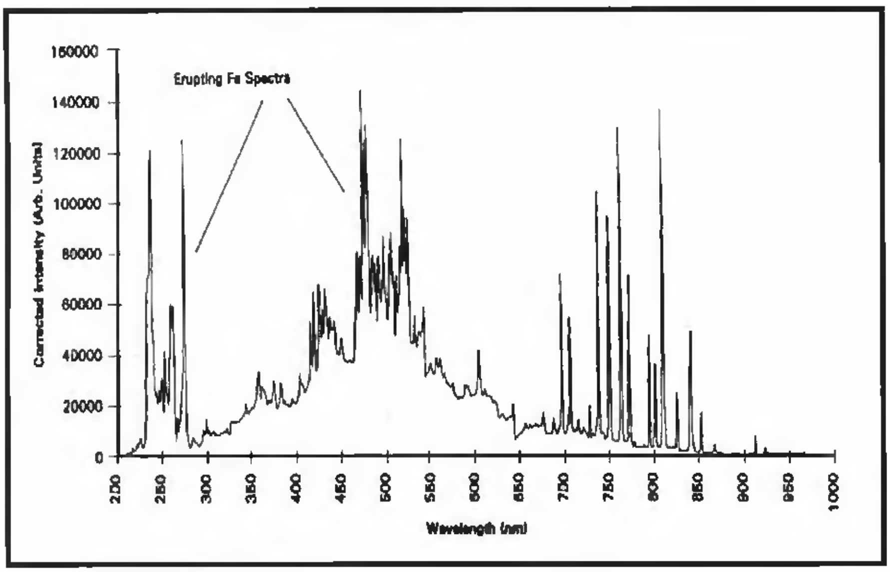

Fig. 3 — Typical gas tungsten arc spectra.

this treatment. The surface of the copper anode was relatively flat, but was unpolished and oxidized.

The nominal welding conditions are shown in Table 1. In some experiments, the conditions varied from these nominal parameters as noted.

Table 1 — Welding Conditions

Electrode	3/16 in. tungsten 2% thoria
Shielding Gas	Argon, 25 ft^3/h
Torch Speed	2 mm/s
Welding Current	100 A DC
Arc Length	2 mm

Experimental Procedure, Results and Discussion

A variety of experiments were performed to provide information needed to design and calibrate the IR temperature measurement system. Principal issues were band-pass filtering of the sensed radiation, quantification and mitigation of interference from the welding arc and correlation of sensing system output to workpiece temperature.

Effect of Band-Pass Filtering

Based on the typical emission spectrum of the gas tungsten arc and the Planck's Law emission of the hot base material, a band-pass filter at 1064 nm with a bandwidth of 15.2 nm was selected to reject radiation from the gas tungsten arc. A series of welding experiments were performed on AISI 1250 steel (prepared as described in the previous section) to quantify the effects of this filter. In these experiments, a normal gas cup (with no shield to shadow the sensing point) was used.

Typical results are shown in Fig. 5A (without filter) and Fig. 5B (with filter). In both the filtered and unfiltered cases, the optical power curve could be divided into four regions:

Region 1: The first region is the arc start area where the optical power increased abruptly at the arc-starting point and then immediately dropped to a lower value. This phenomenon possibly was due to a current surge and/or reflection of arc radiation from a carbon rod used to start the arc. In Fig. 5, the optical power radiated from the arc was taken as the value at the end of the startup "spike." Because the tungsten and workpiece were both still relatively cool at this time, it was assumed that all measured power was radiated by the arc. The optical power from the arc was 1.487 µW in Fig. 5A (unfiltered) and 0.016 µW in Fig. 5B (filtered). It was concluded that the optical filter blocked out a considerable amount of the arc light radiation.

Region 2: In the second region of both the filtered and unfiltered cases, the optical power increased rapidly at first. It then approached a local maximum after about 8~10 s, where it remained nearly constant for a time. This corresponds to the period of time between the initial startup transient and about 200 time units on the plots in Fig. 5. The rise appears to be exponential, consistent with the typical temperature response curve of a heated mass. Within this region, the temperature of the electrode should increase quickly from room temperature up to a possible temperature of above 3000°C (5432°F) due to the electrical resistance and arc heating. Hence, some of the increased optical power in this region was attributed to thermal radiation from the electrode. However, because the temperature of the sensing spot on the base metal also may have increased slightly during this period, it remained to be determined exactly how much of the measured radiation was emitted by the hot electrode and how much by the base metal.

Region 3: In the third region of both plots (extending from roughly 200–500 time units), the optical power again increased rapidly and leveled off at another maximum value. This was thought to be primarily due to temperature rise of the base metal at the sensing point.

Region 4: In the fourth region of the sensor output (from roughly 500 time units to arc shutoff at about 750–800 time units), the optical power was nearly constant with small fluctuations. This was thought to be indicative of the nearly stationary temperatures of the sensing spot and tungsten electrode.

At the end of the fourth region, where the arc was terminated, the measured radiation decreased to zero. The fall time (90–10%) of this decay (which represents the cooling time of the arc, electrode and base metal) was estimated as approximately 5 s — Fig. 5B.

In the unfiltered case (Fig. 5A) the total optical power was about 2.85 μW, including 1.487 μW from the arc (measured at the end of Region 1). Thus, it was concluded that the radiation from the arc would significantly affect the temperature measurement if no band-pass filtering were used. However, in the filtered sensor output (Fig. 5B) the optical power in Region 4 was about 0.156 μW, including 0.016 μW from the arc. It was concluded that the radiation from the arc would have a smaller, but still negligible, affect

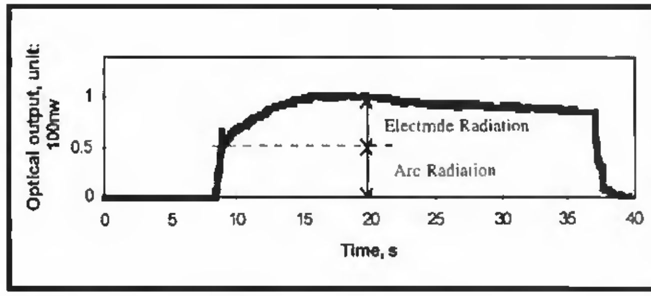

Fig. 6 — Experiments on a water-cooled copper anode with 2-mm arc length.

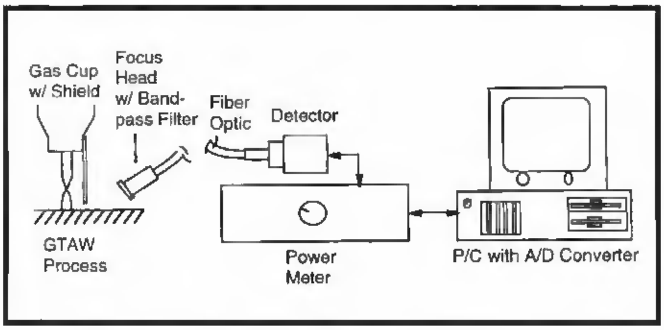

Fig. 4 — Schematic of temperature measurement system.

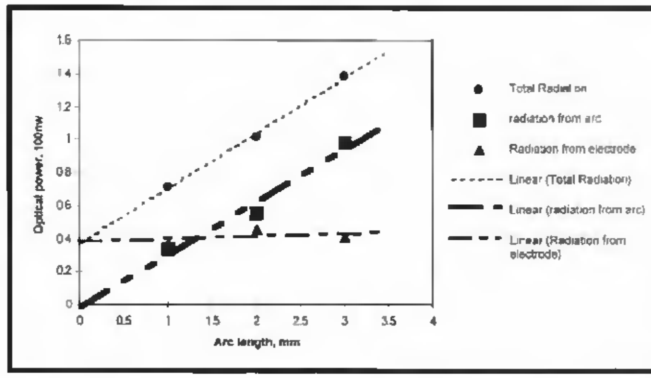

Fig. 7 — Experimental results by varying arc lengths at a welding current of 100 A.

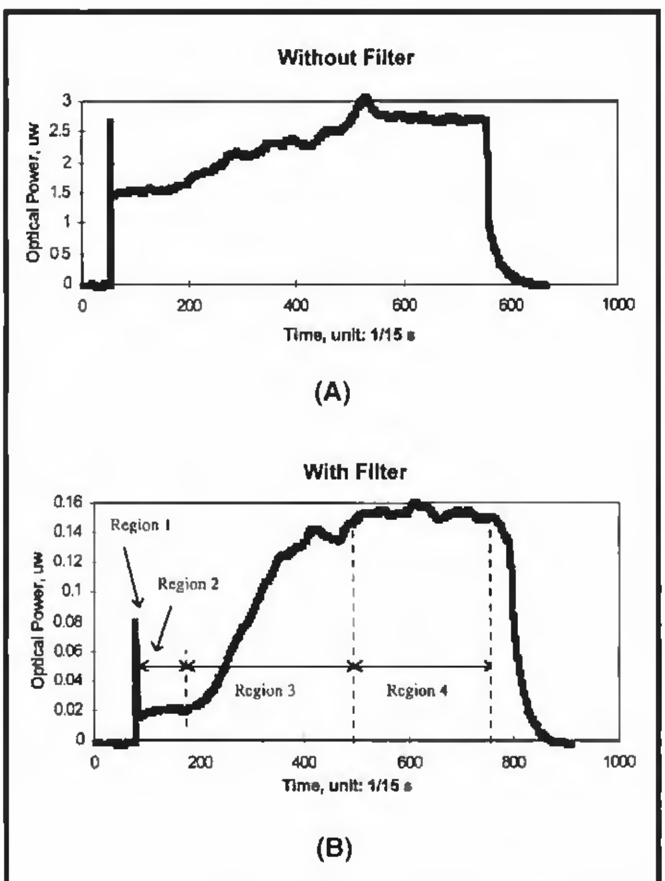

Fig. 5 — Typical sensor outputs with and without band-pass filtering. A — Experimental results without filter; B — experimental results with filter (Note: the vertical axis scale is different than shown in [A]).

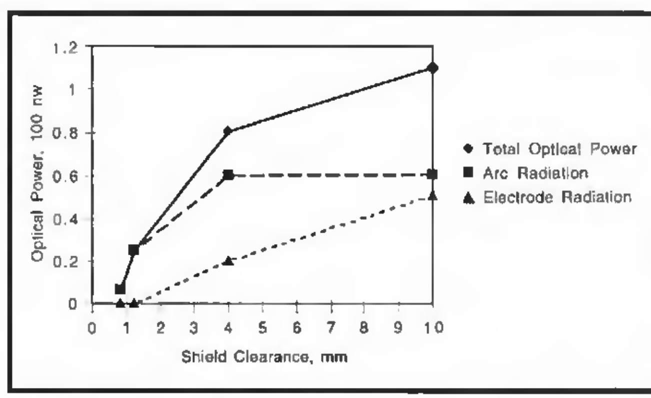

Fig. 8 — Variation of measured optical power with gas cup shield clearance.

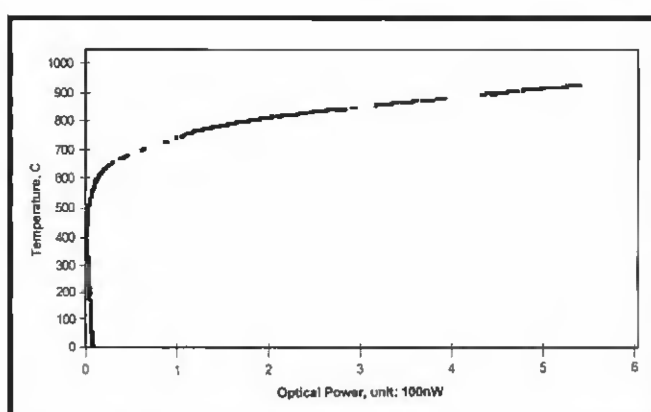

Fig. 9 — Average calibration experiment results.

on the temperature measurement if the optical band-pass filter was used.

As discussed above, three radiation sources contributed to the measured optical power: the welding arc, the electrode tip and the sensing spot on the base metal. It was concluded that the optical filter could block out a large portion of the arc light radiation. However, the remaining arc optical power would have a deleterious affect on low-temperature measurements. It also remained to be determined how much radiation was emitted by the hot electrode.

Experiments on Water-Cooled Copper Anode

Because the initial series of experiments did not quantify the effect of tungsten electrode radiation on the infrared temperature measurements, further experiments with the band-pass optical filter were designed and performed over a water-cooled copper anode. This was done to eliminate the radiation from the sensing spot on the base metal. The water-cooled copper block would remain very cool relative to the steel specimens used in the previous tests. Thus, no measurable thermal radiation would be directly radiated from the sensing point and only the optical power contributed by the arc and electrode would be measured. By analyzing the experimental results, the effect of radiation from the electrode could then be determined.

The first series of experiments using the water-cooled copper anode were performed by varying arc length. Lengths of 1, 2 and 3 mm were used. It was assumed that the proportion of arc radiation measured by the sensor should increase with arc length because arc radiation emitted at increased distances above the plate surface has a more direct specular angle into the sensor. As a result, the effect of the radiation from the electrode and arc could be quantified by varying arc length systematically. The other welding parameters were maintained the same as in the previous experiments on steel. A typical result for a 2-mm arc length is shown in Fig. 6. The measured optical power was much less than that of the previous experiment.

In Fig. 6, the optical power increased abruptly at the instant of arc start. This transient phenomenon is similar to that observed during the first experimental series. Since the copper block remained relatively cool, it was certain that all measured optical power, except that from the arc, was contributed by the electrode and the arc. About eight seconds after the arc start, the optical power from the electrode reached a peak and then declined somewhat until the weld was terminated by extinguishing the arc. This decrease in radiation possibly was due to the small changes of the surface condition of the electrode and/or the copper block. After termination of the arc, the radiation decreased to about zero over a period of approximately 1 s.

To more clearly identify the source of measured radiation (whether from arc or electrode), the data was plotted as radiation power vs. arc length, as shown in Fig. 7. As indicated, the total radiation curve was extrapolated to zero arc length to find the amount of electrode radiation. However, another value for the electrode radiation could also be obtained for each point in Fig. 7 by subtracting the total radiation value immediately after the startup transient (assumed to be solely arc radiation) from the maximum value attained later (assumed to be due to hoth the electrode and arc). As calculated in Fig. 7, the total radiation and arc radiation both increased almost linearly with the arc length. The plot also shows that the value for electrode radiation obtained by extrapolating the radiation vs. arc length curve to zero arc length agrees very well with the value obtained from the individual data sets.

By comparing Figs. 5B and 7, the radiation from the electrode and arc was still a significant fraction of the radiation assumed to be emitted by the base-metal sensing point, even with the optical band-pass filter installed. This motivated the implementation of a shield to block the arc and electrode radiation, described in the next section.

Shield for Blocking Arc Light and Tungsten Radiation

To shadow the sensing point from radiation emitted by the electrode and arc, a sheet-metal shield was designed as shown in Fig. 4. Shield design test experiments were performed over the water-cooled copper anode and the optical band-pass filter was used in all trials. The other welding parameters were set as shown in Table 1.

It is apparent in Fig. 4 that lowering the shield-to-base metal clearance would shadow more arc and electrode radiation from the sensing point. However, for practical reasons of avoiding contact, the clearance should be kept as large as possible. The effect of changing the clearance was ohserved in a series of tests. The experimental results are shown in Fig. 8.

At a clearance of 4 mm, the measured total optical power is almost as large as when no shield was used (corresponding to a shield clearance of 10 mm, the gas-cup-to-work distance). At a shield clearance of 1.2 mm, the measured total optical power was about 20 nW — nearly all of it radiated by the arc. At a shield clearance of 0.8 mm, the measured total optical power and arc power was 6 nW. This measurement is very small compared with that radiated by the sensing spot at nominal welding conditions (*e.g.*, as shown in Fig. 5B) leading to the conclusion that this optical power value would not significantly affect the accuracy of the temperature measurement. It was concluded that a shield clearance of 0.8–1.0 mm provided adequate arc and electrode shadowing for the temperature measurement system. The sheet metal shield was subsequently replaced by a more compact specially-designed gas cup.

Temperature Measurement Calibration

Thermocouple measurements were used to calibrate the temperature sensing system. A series of calibration experiments were performed on AISI 1250 steel prepared as described previously. The welding conditions were as shown in Table 1, except the arc was stationary and current was varied from 60–100 A. The gas cup shield-to-base metal clearance was 1 mm.

The thermocouple wires were welded to the sensing point by a micro-spot-welder. A LabVIEW program in the data acquisition and control computer was used to sample, at a 10 Hz frequency, the voltage signals simultaneously from the thermocouple and optical meter. The samples were converted into temperature and optical power values, respectively. Sampling was started at arc initiation and continued for 60 s, long enough for the signals to stabilize. Thus, a range of calibration temperatures from room temperature up to maximum temperature were recorded for each experiment.

All results were plotted as temperature vs. optical power. In all tests, the thermocouple temperature measurements were within 20°C for any given optical power. All of the experimental results were averaged together and used to plot the calibration curve shown in Fig. 9.

In Fig. 9, the initial optical power was less than 6 nW and decreased to about 2 nW as the temperature increased from room temperature up to about 400°C (752°F). Since the radiation intensity was too low to be detected by the temperature-sensing system at temperatures less than 400°C (752°F), it was concluded that the measured optical power in this temperature range came from the reflection of arc light. Due to the increased temperature, the reflectivity of the base metal decreased. Hence, the optical power also decreased slightly. Above 450°C (842°F), the thermal radiation from the sensing point dominated the optical power (above 6 nW) and the radiation intensity increased rapidly with increasing temperature. The results showed that temperatures above 450°C could be satisfactorily measured by the infrared temperature-sensing system with an accuracy of about ±10°C (±50°F). The average calibration curve was fitted with a mathematical function, valid only for temperatures above 450°C (842°F):

$$T = 92.65 \ \mathrm{Ln}\ (P_{opt}) + 745.31$$

where T is temperature (°C) and P_{opt} is measured optical power (in units of 100 nW). The final result of the experiment is the calibration curve used in subsequent penetration control experiments.

Conclusions

Based on the experiments described above, it was concluded that both arc and electrode radiation interfered very significantly with infrared temperature measurements made at a location on the base metal near the welding arc. A combination of band-pass optical filtering and shielding was necessary to allow accurate infrared measurement of temperature at a location 12 mm behind and 5 mm to the side of the arc centerpoint. It should be noted that the results indicate that pulsing of the arc at typical frequencies used in practice (*e.g.*, 0.1-1.0 Hz) may not have entirely removed the interference, because radiation from the arc and tungsten electrode took approximately 1 s to decay completely after arc termination. The experiments verified that filtering and shielding practically eliminated arc and electrode interference from the infrared thermal measurements. Finally, an experimental calibration of the infrared measurements based on thermocouple measurements was performed.

References

1. Doeblin, E. O. 1975. *Measurement Systems Application and Design*. New York, McGraw-Hill, pp. 540–544.

2. Richardson, R. W. 1996. Arc physics. WE 801 lecture notes, *Welding Engineering*, The Ohio State University.

3. Bicknell, A. 1994. Infrared sensor for top face monitoring of weld pools. *Measurement Science & Technology* 5: 371–378.

4. Chin, B. A., Madsen, N. H., and Goodling, J. S. 1983. Infrared thermography for sensing the arc welding process. *Welding Journal* 62(11): 227-s to 234-s.

5. Lukens, W. E., and Morris, R. A. 1982. Infrared temperature sensing of cooling rates for arc welding control. *Welding Journal* 61(1): 27–33.

6. Parron, B. E. 1971. The mathmatical modelling of welding processes to create systems for forecasting the quality of joints and for optimum control. *Automation*, Vol. 24.

7. Groth, W. G., Ramsey, P. W., and Weiss, M. 1963. Infrared temperature sensing systems for automatic fusion welding. *Welding Journal* 42(8): 337-s to 346-s.

8. Green, D. R., and Hassberger, J. A. 1977. Infrared electro-thermal examination of stainless steel. *Materials Evaluation*.

9. Banerjee, P. 1995. Infrared sensing for on-line weld geometry monitoring and control. *Journal of Engineering for Industry* 117: 323–330.

10. Hand, D. P. 1995. Nd:YAG laser welding process monitoring by non-intrusive optical detection in the fibre optical delivery system. *Measurement Science & Technology* 6: 1389–1394.

11. Nomura, H. 1994. *Sensors and Control Systems in Arc Welding*. Japan, Chapman & Hall.